MICROFLUIDICS

1. Introduction

Microfluidics is a technology that features the movement of small volumes of fluids through channels with dimensions of roughly 1–500 μm. At this size scale, factors that influence the behavior of fluids are different from those at the macroscale; eg, surface forces become an increasingly dominant factor for microscale systems. In practice, microfluidics provides a powerful research platform for studying basic phenomena of fluid flow at the microscale, and a valuable analytical tool for conducting experimental assays.

The modern field of microfluidics originated ∼1990 by Manz and co-workers (1–3). [Work in microfluidics had sparingly appeared before then, such as the fabrication of a gas chromatograph on a silicon wafer (4)]. Today, many different microfluidic devices are being developed, including flow sensors, pressure regulators, integrated systems with pumps and valves, capillaries, and chemical detectors. Although it is possible to fabricate highly elaborate microfluidic devices using traditional micromachining methods on glass and silicon, advances in soft lithography have rendered the fabrication of routine microfluidic devices in elastomers straightforward and inexpensive, thereby spreading the access of this technology to nonspecialists.

Miniaturized versions of assays offer many advantages, including requirements of small amounts of solvents, reagents, and cells (critical for valuable samples and for high throughput screening), short reaction times, portability, low cost, low consumption of power, versatility in design, and potential for parallel operation and for integration with other miniaturized devices. The use of microfluidic technology today allows researchers to investigate new microscale phenomena and engineer powerful "lab-on-a-chip" (LOC) devices. This article discusses the basic features of microfluidics, applications of microfluidics, the spread of the microfluidics technology in industry, and the future challenges of this technology.

2. Basic Features of Microfluidics

2.1. Physics of Fluid Flow.   Microfluidic devices use channels to control the movement of fluids and gases at a size scale of ∼1−500 μm. The scaling of different physical parameters in devices with characteristic size d from 1 mm down to 10 μm is illustrated in Table 1. Benefits from downscaling include a significant reduction in the cost of material and the volume of expensive reagents required to perform analysis, faster reaction rates, and shorter analysis time. Through the process of miniaturization, some physical phenomena that are not important on the macroscale become relevant and even dominate in small dimensions. The factors that govern microfluidics include Reynolds number (Re), laminar flow, diffusion, fluidic resistance, surface area/volume ratio, and surface tension. These properties are described below.

Reynolds Number.   The Re is the ratio between inertial forces and viscous forces acting on the fluid. It is defined as $Re = vl\rho/\mu$, where v is the characteristic

Table 1. **Effect of Scale[a] on a Number of Device Parameters[b,c]**

Device parameters	Characteristic length d		
	1 mm	100 μm	10 μm
volume	10^{-6}L	10^{-9}L	10^{-12}L
number of molecules in a 1 μM solution	6×10^{11}	6×10^8	6×10^5
diffusion time	15 min	10 s	100 ms
arrangement	25 volumes/cm^2	2500 volumes/cm^2	2.5×10^5 volumes/cm^2
maximum information density	1.67 values per min and cm^2	250 values per sec and cm^2	2.5×10^6 values per sec and cm^2

[a]Expressed in terms of a characteristic length d.
[b]This table is adapted from Ref. 5.
[c]"Diffusion time" is the time that a molecule with a diffusion coefficient of 10^{-9} m^2/s needs to travel a distance of 1 mm. "Arrangement" is the maximum number of devices that can be arranged on a surface. A "maximum information density" number is calculated by the number of volumes present divided by diffusion time.

velocity of the fluid (m/s), l is the characteristic length (m) (equal to hydraulic diameter D_h if a cross-section is circular), ρ is the fluid density (for water, 1000 kg/m^3), and μ is the viscosity of the fluid [for water, 10^{-3} kg/(m·s)]. In general, microfluidic devices, with water as the working fluid, velocities of 1 μm/s to 1 cm/s, and typical channel radii of 1/100 μm, the Reynolds numbers (Re) are low and range between 10^{-6} and 1. In channel flows, a Re < 2000 typically indicates laminar flow, whereas flows with Re > 3000 tend to be turbulent (Fig. 1). The transition zone between the two levels may be either laminar or turbulent.

Laminar Flow. Laminar flow is a phenomenon in which fluids flow side-by-side with no turbulent mixing between the fluid streams. In laminar flow, mixing between the fluid streams occurs only by diffusion across the boundary. Since laminar flow takes place at low Reynolds numbers, the small size of microchannels typically gives rise to laminar flow condution. Laminar fluid flow is described by the limiting form (for values of Re < 10) of the Navier-Stokes equations known as the Stokes equation (6,7). For cases of inviscid flow, the Bernoulli equation can be used to describe the flow. The prevalence of laminar flow in microfluidics has given rise to new technologies. For example, Yager and
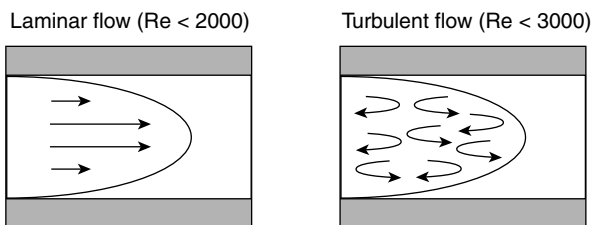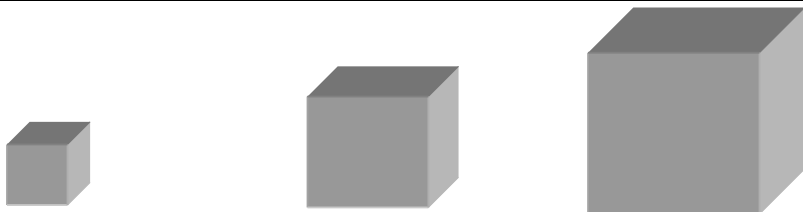

Fig. 1. Schematic representations of laminar and turbulent flow. Arrows represent the movement of fluid elements.

co-workers used diffusion at the boundary as the basis for an immunoassay (8,9). Whitesides and co-workers demonstrated membraneless electrochemistry using the slowly diffusing boundary as a barrier, and microfabrication at the boundary using multiphase laminar flow patterning (10–13).

Diffusion. Diffusion is the random migration of molecules or small particles arising from motion due to thermal energy. The time for diffusion in one dimension (1D) can be modeled by the equation $t = d^2/2D$, where d is the distance that a particle moves (in cm) during a time period t (in s), and D is the diffusion coefficient of the particle (for most proteins, between 10^{-6} and 10^{-7} cm^2/s) (14). Since the diffusion distance d is usually short in microchannels (µm), the diffusion time t is therefore correspondingly small. Maximizing the interfaces between two mixing solutions (eg, by stretching and folding the fluid elements) within the microchannel allows diffusion to occur more rapidly.

Fluidic Resistance. The governing equations of fluidic resistance in microchannels are well defined (6). Analogous to electrical resistance, which is equal to the ratio of potential difference to current, fluidic channel resistance R (Pa·s/m^3) within a microchannel is the ratio of pressure difference ΔP cross the channel (Pa) overflow rate Q (m^3/s), ie, $R = \Delta P/Q$. For circular microchannels, the fluid channel resistance is calculated using the formula $R = 8\,\mu L/\pi r^4$, where µ is fluid viscosity (Pa·s), L is the channel length (m), and r is the channel radius (m). A remarkable consequence of this relation is that the resistance of a channel scales inversely to the forth power of the cross-sectional radius, such that the resistance of a 10-µm channel is 10,000 times higher than that of a 100-µm channel, given that other parameters remain constant. For a rectangular microchannel, if this microchannel is of low aspect ratio (ie, $w = h$), the fluidic channel resistance can be calculated by $R = (12\,\mu L/wh^3)\{1 - (h/w)[(192/\pi^5) \sum_{n=1,3,5}^{\infty}(1/n^5)\tanh(n\pi w/2h)]\}^{-1}$. Conversely, for a rectangular microchannel with a high aspect ratio (ie, $w \leq h$ or $h \geq w$), the resistance can be found by $R = 12\,\mu L/wh^3$, where w is the channel width (m) and h is the channel height (m). A long narrow channel therefore exhibits high fluidic resistance, while a short wide channel exhibits low fluidic resistance. From the previous equation, the dominant geometrical contribution to viscous resistance originates from the shortest cross-sectional length. Bruus and co-workers examined Hagen-Poiseuille flow in microchannels with different cross-sectional shapes, and determined the dependence of hydraulic resistance on the shape of the channel (15). See (16,17) for the formula for other channel geometries and their corresponding fluidic channel resistances.

Surface Area/Volume Ratio. The surface area to volume (SAV) ratio describes the curvature of an interface. Surface forces dominate the flow behavior within microchannels. For example, the SAV ratio for a device with a characteristic length of 1 m is of order 1 m^{-1}, compared to the SAV ratio for a microfluidic device (having a characteristic length of 10 µm) of 10^5 m^{-1} (Table 2). This large difference in SAV is significant in the consideration of a number of parameters, since some parameters (eg, surface tension, pressure, shear stress) scale with the surface area of the fluid, whereas other forces (eg, gravitational, electrical, dielectrophoretic, inertial) scale with the volume of the fluid. With an increase in the SAV ratio, surface forces as shear stress, surface tension, and pressure increase in influence.

Table 2. **Scaling of the SAV Ratio for Cubes of Different Sizes**

Object	1-μm cube	1-mm cube	1-m cube
surface area	$6 \text{ sides} \times (10^6\text{m})^2$ $= 6 \times 10^{12}\text{m}^2$	$6 \text{ sides} \times (10^3\text{m})^2$ $= 6 \times 10^6\text{m}^2$	$6 \text{ sides} \times (1\,\text{m})^2$ $= 6\,\text{m}^2$
volume	$(10^6\text{m})^3 = 10^{18}\text{m}^3$	$(10^3\text{m})^3 = 10^9\text{m}^3$	$(1\,\text{m})^3 = 1\,\text{m}^3$
SAV ratio	6 million m^{-1}	6000 m^{-1}	6 m^{-1}

Surface Tension. The surface tension γ (N/m) is the magnitude F (N) of the force exerted parallel to the surface of a liquid divided by the length L (m) of the line over which the force acts (ie, $\gamma = F/L$). It describes the tendency of liquids to reduce their exposed surface to the smallest possible area as the result of cohesion between liquid molecules at the liquid–gas interface. Microfluidic systems can exploit surface tension to transport immiscible liquid at different flow rates; in a simple example, fluid travels up a thin capillary. In a network of channels, surface tension effects can be exploited to move the fluid into desired channels. For example, the technique of electrowetting can be performed by applying an electric charge via an electrode to the surface of a channel to change the surface tension between the inner wall of a channel and the fluid within (18). The reduced surface tension in one portion of the channel draws the fluid to flow toward that direction (19). Electrowetting can also be performed by applying an electric field to one side of a droplet to lower its surface tension and to flow in that direction (20).

Fluid Flow. There are two main methods for driving fluids and particles in microchannels: pressure driven and electrokinetic. For pressure-driven flow (also called hydrodynamic flow), the flow rate Q (m^3/s) is given by $Q = \Delta P/R$ (see the section FLUIDIC RESISTANCE), and the pressure drop can be created either by opening the inlet to atmospheric pressure and applying a vacuum at the outlet, or by applying positive pressure at the inlet (eg, via a syringe pump) and opening the outlet to atmospheric pressure. Pressure-driven flow results in a parabolic flow profile (Fig. 2**a**). Electrokinetic flow is based on the movement of molecules in an electric field due to the interaction of their charges with an external electric field. There are two components to electrokinetic flow: electrophoresis, which results from the accelerating force due to the charge of a molecule in an electric field balanced by the frictional force, and electroosmosis, which creates a uniform plug-like flow of fluid down the channel (Fig. 2**b**). For electrokinetic flow, small channels have the advantage of a high SAV ratio, and thus dissipate heat more efficiently than large channels. [At running voltages of tens of kilovolts, the flow of electric current through the buffer produces a significant amount of joule heat, which results in an increase in temperature in the microcapillary, and subsequently the production of microbubbles and broadening of the travelling
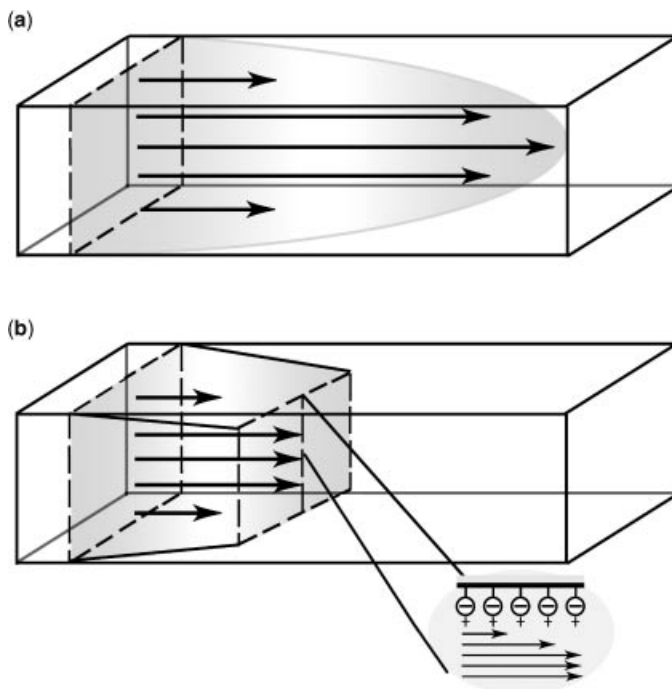
Fig. 2. Schematic representations of flow profiles of (**a**) pressure driven and (**b**) electro-osmotic flow. In both figures, the arrows show the direction of fluid flow. In (**b**), the schematic diagram shows a negatively charged surface (eg, glass). In reality, the surface can be either positively or negatively charged to support electroosmosis.

bands of analytes (21).] [See review by Stone and co-workers for an overview on electrokinetic fluid flow in microfluidics (27).] For both pressure-driven and electroosmotic flow, the "no-slip" boundary condition is thought to apply, such that fluid flow right at the surface is zero. Fluid flow in microchannels using other principles has been described. Delamarche and co-workers (22) used capillary action in plasma-oxidized poly (dimethylsiloxane) (PDMS) to deposit immunoglobulins onto a surface. Centrifugal force was used to drive fluid flow in PDMS channels on a plastic disk, on which enzymatic assays were performed (23). In non-PDMS-based systems, fluid flow was directed using gradients in surface pressure due to redox-active surfactants (24), gradients in temperature (25), patterns of self-assembled monolayers with different surface free energies, and capillary action (26).

2.2. Fabrication of Microfluidic Structures. The most commonly used materials for microfludic systems are silicon, Pyrex glass, and elastomers. We describe the fabrication of microfluidic structures using these materials in the following section.

Silicon. Microfluidic devices fabricated from silicon are commonly used for MEMS (micro-electromechanical systems) technologies, which integrate mechanical elements, sensors, actuators, and electronics into complete lab-on-a-chip systems. The electronic components are fabricated using integrated circuit (IC) processes (eg, CMOS, bipolar, or BICMOS processes), and the

micromechanical components are fabricated using compatible "micromachining" processes that selectively etch away parts of the silicon wafer or add new structural layers to form the mechanical and electromechanical devices. In the end, MEMS enable the development of devices with the computational performance of microelectronics and the perception and control capabilities of microsensors and microactuators.

There are at least three categories of technologies for the fabrication of MEMS devices (28): bulk micromachining, surface micromachining, and high aspect ratio micromachining (HARM). Bulk micromachining is a subtractive process that involves the selective removal of the wafer substrate material to form the MEMS structure, which can include cantilevers, holes, grooves, and membranes. Surface micromachining is an additive process that involves depositing combinations of thin structural and sacrificial layers, wherein the sacrificial layers are subsequently removed to form raised structures that can include gears, comb fingers, cantilevers, and membranes. HARM includes deep ultraviolet (uv) or X-ray lithography techniques known as LIGA (from the German Lithographie, Galvanoformung, Abformung, meaning lithography, electroplating, and molding). LIGA allows researchers to create microcomponents out of polymers, metals, and ceramic materials using micromachined molds (29).

Pyrex Glass.   A silanol-rich material, eg, glass, is the preferred substrate material for electrokinetically driven microfluidic systems. A detailed description of the fabrication procedure is presented in Ref. 30, and the basic processes are briefly summarized as follows: The glass is first annealed at 400°C for 4 h in order to release residual stress before the fabrication process. Then the glass is cleaned through immersion in a boiling piranha solution (concentrated sulfuric acid mixed with concentrate hydrogen peroxide, in 3:1 volume ratio) for 10 min. A schematic representation of a sample fabrication process is presented in Figure 3**a**. Initially, a thin layer of AZ 4620 photoresist, is applied onto the glass substrate, and then patterned using a standard photolithography process. The patterned photoresist layer is hard-baked, and used directly as a mask in the etching of the glass substrates in a commercially available buffered HF (buffered oxide etchant) for 45 min. The etched glass substrates are then immersed in a diluted KOH solution to remove the photoresist layer. In a separate process, holes for input and output of fluids are drilled in a second bare glass. Both glass substrates are cleaned in a boiling piranha solution, and then carefully aligned. Finally, the substrates are fusion bonded in a sintering oven at a temperature of 580°C for 10 min. The entire fabrication process lasts ~10 h. A glass chip is shown in Figure 3**b**.

Poly(dimethylsiloxane).   Due to its amenability for rapid prototyping, the poly(dimethylsiloxane) (PDMS) elastomer is one of the most widely used polymers in microfluidic applications to form components, such as channels and valves. As a material, PDMS offers many advantages: it is optically transparent; it can be easily processed by molding and acquired at low costs; it is elastic; and it can form fluid seals effectively.

Procedures for the fabrication of PDMS structures for microfluidics (Fig. 3**c**), as pioneered by Whitesides and co-workers, are described in detail elsewhere (31−33). Briefly, a photomask pattern is made in a computer-aided design (CAD) program. The CAD-generated patterns are printed onto transparencies
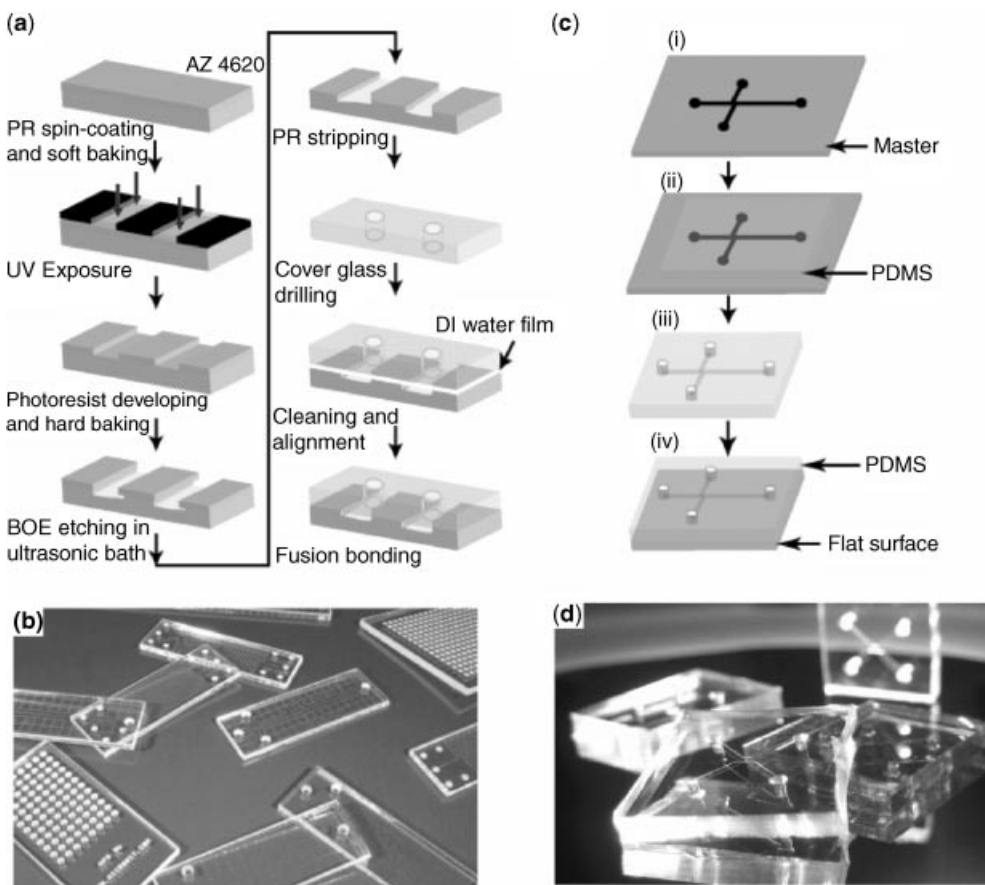
Fig. 3. Fabrication and pictures of microfluidic devices made of different materials. (**a**) Procedure for fabrication of glass microchannels (30). (**b**) Photograph of glass CE chip from Micronit Microfluidics BV, The Netherlands. (**c**) Procedure for fabrication of PDMS microchannels: (*1*) Fabricate master by rapid prototyping; (*2*) Cast prepolymer and cure; (*3*) Remove PDMS replica master and punch holes for inlets and outlets; and (*4*) Oxidize PDMS replica and flat in plasma and seal to a flat surface. (**d**) Photograph of microfluidic chips made of PDMS.

using commercial services with overnight turnaround times. Lateral resolutions of 8 μm can be achieved using photoplotters operating at 20,000 dots per inch (34). (For features beyond 8 μm, chrome masks can be used, but they take longer to fabricate commercially, and are more expensive than transparencies.) Photoresist, such as SU-8, is spin-coated on a clean silicon wafer at different speeds to achieve thicknesses ranging from 1 to 300 μm. The photomask is placed over the photoresist; together, they are exposed to uv light. A developing reagent is used to dissolve the uncrosslinked regions, and the resulting bas-relief structure serves as a master for fabricating PDMS molds. To create the PDMS mold, the prepolymer is mixed with the curing agent at a 10:1 weight ratio, poured over the master, and degassed. (The masters may also be treated with fluorinated silanes beforehand to decrease adhesion to PDMS.) The PDMS is cured at 70°C for at

least 1 h, and peeled from the master to produce the final replica bearing the designed microstructures. Using a borer or needle, small holes are drilled into the PDMS to produce inlets and outlets. Finally, the PDMS replica is sealed to a flat surface to produce the microfluidic device. The PDMS can seal to itself and other flat surfaces reversibly by conformal contact (via van der Waals forces). If both surfaces are silicon-based materials, each surface can be oxidized by plasma before contact to achieve an irreversible seal via covalent $O-Si-O$ bonds. This whole procedure from CAD to the fabrication of the final device can be performed in <24 h. Making PDMS replica molds of microfluidic devices from masters requires only a few hours.

As the material of choice for microfluidic systems, polymers, eg, PDMS, exhibit advantages over silicon and glass, because they are easy to fabricate, and are compatible with the requirements of many bioassays. The PDMS-based microfluidic systems can be used as a useful step to test new designs, or as a final product, as shown by a number of functional devices developed in academic institutions and private companies. Some disadvantages of PDMS include: hydrophobicity of its surface, which resists wetting by aqueous solutions and is prone to nonspecific protein adsorption (necessitating in some cases surface modification); incompatibility with high concentrations of some organic solvents (35), which may otherwise be useful in some assays (eg, liquid chromatography); and limitations of feature geometries (its elasticity limits the aspect ratios of the features due to shrinking or sagging). Other polymers, eg, polyurethanes (36) and fluorinated polymers (37) are often used to construct microfluidic devices. Poly(methyl methacrylate) (PMMA) is a clear plastic (often used as a shatterproof replacement of glass) that is also commonly used for microfluidic systems (38).

3. Applications of Microfluidics

3.1. Physics.   Flow of fluids in microchannels is usually laminar due to the low Re inside a microchannel. As a result, it is challenging to mix fluids inside microchannels. To enhance the rate of mixing, transverse flows can be generated to transport solutes over the cross-section of the channel. There are two strategies for generating such transverse flows: passive mixers that have no moving parts and that achieve mixing with only the design and topology of the channels, and active mixers, which either have moving parts or use externally applied forces, eg, pressure or electromagnetic fields (39). Examples of passive mixers include the design of channel geometry to promote chaotic advection; this process leads to an increase in the interfacial area, and subsequently greater diffusive mixing (Fig. 4). This type of passive mixer can be used to generate well-controlled gradients of molecules (41). In another implementation of a passive mixer, the addition of a small amount of deformable high molecular weight polymers to a liquid inside a curved microchannel generates elastic stresses, leads to instabilities and irregularities of the flow, and enhances the mixing in a channel (42). In a T-junction design, bubbles can also be used to mix reagents in microchannels (43).

Active mixers can be classified according to presence of moving parts. Examples of micromixers with moving parts (that can either rotate or oscillate) include
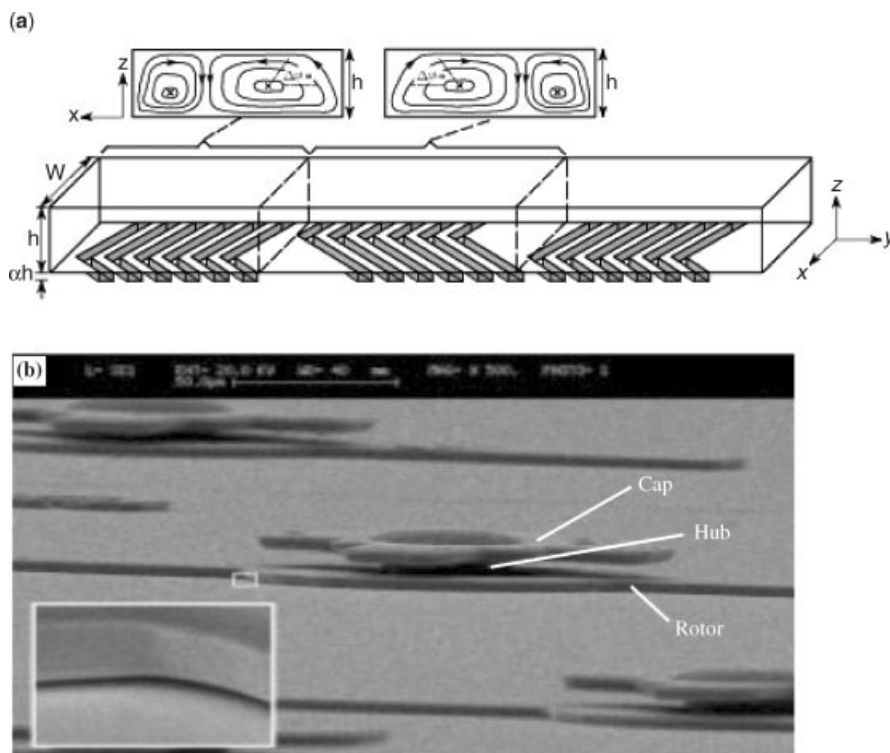
Fig. 4. Passive and active mixers. (**a**) Schematic diagram of a staggered herringbone mixer (SHM), Ref. 41. A mixing cycle is composed of two sequential regions of ridges. (**b**) An active magnetic microstirrer for microfluidic mixing. [Reprinted with permission from IEEE (40).]

microscopic stir bars, piezoelectric membranes, and gas bubbles. A micrograph of a magnetic stir bar is shown in Figure 4**b**. Examples of micromixers without moving parts include magnetohydrodynamic (MHD) convection (39), electrohydrodynamic (EHD) convection (44), and electrokinetic instability (45). [For a greater discussion on the physics of microfluidics see review by Squires (46).]

Precise manipulation of minute amounts of reagents can be achieved by confinement within droplets in an immiscible carrier fluid (47). Such techniques of multiphase flows in microfluidics can be used to aliquot precise amounts of fluids, and mix multiple fluid components with minimal consumption of reagents.

3.2. Chemistry. Microfluidic systems may be used to control chemical reactions in space (microns) and time (milliseconds). The reaction time of diffusion-limited reactions can be controlled by injecting two fluid streams (each containing a different reactant), and spatially varying the points at which the fluid streams converge (which represents the initiation of a chemical reaction) and diverge [which represents the termination of the reaction (48)]. The reaction times can be changed further by varying the flow velocity. Some problems associated with this method include inefficient mixing due to slow diffusion in

laminar flow, and inhomogeneous mixing due to the uneven broadening of the interface between two liquids (49). To overcome these problems, Ismagilov and co-workers developed a simple two-phase system that used aqueous plugs separated by water-immiscible oil (50). Since the plugs moving in straight channels generated a steady, recirculating flow, this design eliminated dispersion and promoted chaotic advection to achieve rapid mixing. These types of systems may prove useful for chemical analysis, synthesis, and complex reaction networks.

Microfluidics may also be used to create linear temperature gradients across a planar surface. By arranging a linear array of microfluidic channels between a heat source and sink on a chip, a temperature gradient can be created. This setup allows one to obtain, in a high throughput manner, activation energies of catalytic reactions, melting point transitions of lipid membranes, and fluorescence quantum yield curves of semiconductor nanocrystal probes as a function of temperature (51). In another application, Cremer and co-workers devised a planar microfluidic device with a series of parallel microchannels perpendicular to a temperature gradient (52). Since each channel was held at a discrete temperature, one could obtain a melting curve of double-stranded DNA (dsDNA) simply by collecting data from all the channels.

3.3. Biological Studies.   To build a functional microfluidic bioassay, it is beneficial to integrate components, such as pumps, valves, reservoirs, and diodes. This section describes examples of functional microfluidic devices for applications in biology. Such devices are useful in detection, separation, and cell sorting.

Immunoassays.   Immunoassay is a principal method of diagnosing diseases by detecting analytes using antibodies. Most immunoassays are heterogeneous: the antigen−antibody complex is bound to a solid substrate, and free antibodies are removed by washing. By contrast, the free and bound antibodies in homogeneous immunoassays do not need to be separated via a solid substrate. Although homogeneous assays minimize washing steps and fluid handling, they require that the free and antigen-bound antibodies exhibit different electrophoretic mobilities. More work has been done on miniaturizing heterogeneous immunoassays than on homogeneous immunoassays. Disadvantages of heterogeneous immunoassays (eg, enzyme-linked immunosorbent assay, or ELISA) in microtiter wells are that they require considerable time to perform and involve labor-intensive handling procedures. Incubation times take hours to allow diffusion of the analyte from the solution to the surface.

Microfluidics shortens the incubation times needed for surface events by minimizing the diffusion distance in microchannels, and replenishing the diffusion layer with a fixed concentration of molecules from active fluid flow. In one microfluidic immunoassay, the device automatically serially diluted the sample and presented multiple antigens on the surface for analysis (31). The device employed a microdiluter network that mixed the sample with buffer using a chaotic mixer.

In another method based on patterning lines of antigens onto a surface (PDMS substrate), the micromosaic immunoassay (Fig. 5**a**) uses one microfluidic network to direct the immobilization of antigens, and a second orthogonal network to direct the flow of samples. Mosaic-format immunoassays may allow samples to be screened in a combinatorial fashion with the advantages of reagent
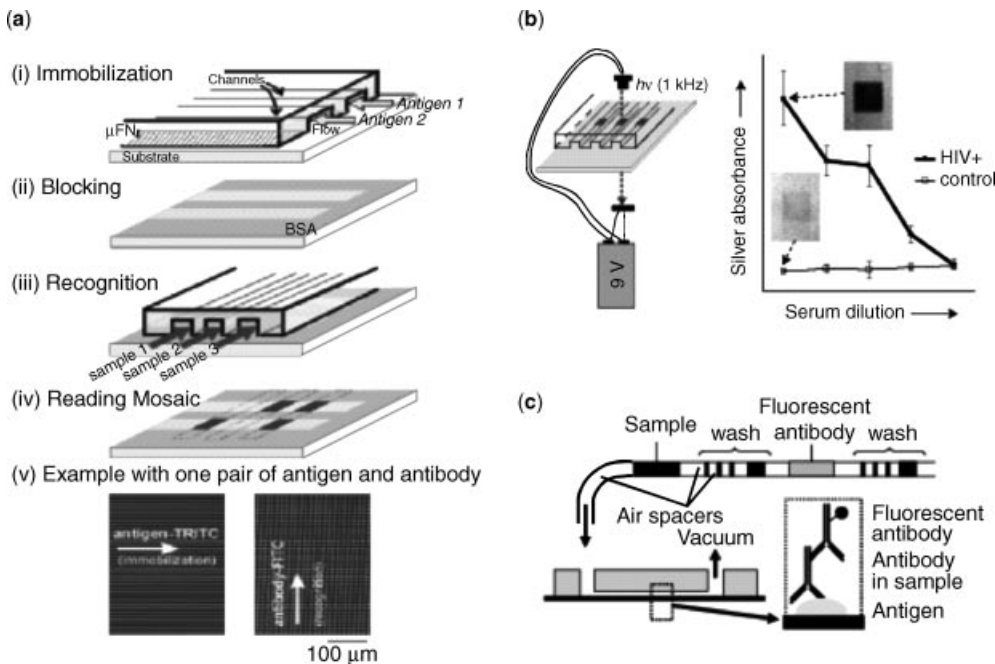
Fig. 5. Immunoassays. (**a**) Strategy for performing a micromosaic immunoassay. (*1*) Different antigens are patterned along single lines. (*2*) The area of substrate that is unpatterned in step (*1*) is coated with BSA to block nonspecific binding of proteins. (*3*) Antibodies flowing through a second microfluidic network bind to the patterned antigens. (*4*) Reading the binding mosaic shows the amount of antibodies in the sample. (*5*) The mosaic can be read by using a fluorescent microscope. [Reprinted with permission from the American Chemical Society (53).] (**b**) Schematic representation and titration curve of POCKET (*po*rtable and *cost effec*tive) immunoassay, a portable and low cost immunoassay for resource-poor settings (54). (**c**) Schematic representation of a reagent-loaded cartridge for valveless and automated fluid delivery in microfluidic devices. [Reprinted with permission from the American Chemical Society (55).]

economy and reduced analysis times. For micromosaic immunoassays, optimal detection occurred in real time and took ∼10 s for surfaces with high density of analytes (53).

Researchers have also developed methods to make microfluidic immunoassays available to resource-poor settings. The "POCKET immunoassay" ("POCKET" short for *po*rtable and *cost-e*ffective) (Fig. 5**b**) shows a comparable analytical performance to that of ELISA with the added benefits of low cost, speed, and portability. The use of gold-conjugated antibodies followed by silver development allowed one to measure the signal in a microchannel using a low cost detector. This system can potentially be combined with a passive method of delivering a series of multiple reagents to build an integrated, low cost, immunoassay for resource-poor settings (Fig. 5**c**).

Electrophoresis. Analytical techniques, eg, capillary electrophoresis (CE) (56) and liquid chromatography can be performed on a microfluidic chip to separate proteins and DNA. In most microchip formats, the micromachined channel serves as the separation column. Analysis of various substances,

ranging from small drug molecules, amino acids (57), peptides (58), and oligo-nucleotides (59) to large proteins (60) DNA fragments (61) and lipoproteins (56) have been demonstrated with electrophoresis on microchips. Capillary electro-phoresis is a popular technique for miniaturization onto a chip because of the ease with which fluid flow can be controlled electrokinetically. Glass-based chips are most common since glass tends to support electroosmotic flow better than PDMS. Also, since the electroosmotic flow of glass is similar to that of fused-silica, transferring separations from CE to on-chip electrophoresis is easier with glass than with PDMS (62). Reversed-phase HPLC of peptides and proteins has been performed on a microchip that integrates subnanoliter on-chip injection and separation (63). (Note that the difficulty in miniaturizing high pressure systems for driving fluid flow in packed columns has limited the work on miniaturizing liquid chromatography; see (64) for a discussion of recent work.)

The small volume of injected sample plugs in on-chip electrophoresis results in fast separation, whereas the use of microfluidics offers process integration, parallel analysis, and high throughput (65,66). Additionally, short separation channels lower the voltage requirement for electrophoresis on microchips. Never-theless, analytes that exhibit similar electrophoretic mobilities can remain unre-solved, as the operation of the device is limited by joule heating, and hence by the maximal voltage that can be applied (67).

A significant difference between conventional CE and electrophoresis in microfluidic chips is the method for injection of samples. In on-chip electrophor-esis, sample injection is achieved through a tee-injector design (68,69). Since the first demonstration of on-chip electrophoresis, the width of sample channels for cross and tee injectors have been reduced to improve resolution, column effi-ciency, and sensitivity (70).

Two-dimensional (2D) separation systems use an open-channel electrochro-matography as the first dimension and capillary electrophoresis as the second dimension. The design features a separation channel with spiral geometry for open-channel electrochromatography coupled to a straight separation channel for CE. Analysis of fluorescently labeled products from tryptic digests of β-casein took 13 min in the 2D electrochromatography–CE system (71). Glass-based microchips can also be used to separate low density lipoproteins. Verpoorte and co-workers demonstrated the separation of low and high density lipoproteins (LDL and HDL respectively) by adding sodium dodecyl sulfate (SDS) to the sam-ple prior to injection (56). Santiago and co-workers developed an acrylic micro-fluidic device that sequentially coupled isoelectric focusing (IEF) and capillary electrophoresis for multidimensional separation of proteins (72).

PDMS can be easily molded to form channels for the separation of biological molecules. Plasma oxidation of PDMS surfaces changes its hydrophobic surface properties by generating silanol groups that are negatively charged at neutral or basic pH. This charged surface, in turn, enables electroosmotic flow toward the negatively charged cathode (31). Native PDMS channels (ie, PDMS channels that are not modified) can also be used for electrophoresis. In an initial demon-stration of capillary electrophoresis in PDMS microchannels, Effenhauser and co-workers (73) achieved efficient separation of DNA fragments in native PDMS channels using electrokinetic flow in a sieving matrix. For field strengths

$<1\,$kV/cm, joule heating was effectively dissipated by PDMS. Morever, Harrison and co-workers (74) showed that native PDMS could also support a reproducible and stable electroosmotic flow (the origin of the surface charge may stem from silica fillers in the polymer). The ability of oxidized and native PDMS to support electroosmotic flow may depend on the ionic strength of the buffer (75). To characterize the electrokinetic properties of PDMS microchannels, Thormann and co-workers compared electroosmosis and current density obtained in reversibly sealed PDMS/PDMS and hybrid PDMS/glass channels to those obtained in a fused-silica capillary. Compared to fused silica, electroosmotic flow in PDMS/PDMS and PDMS/glass microchannels is significantly (50–70%) lower. Only at $pH \geq 6.4$ is the electroosmotic flow in PDMS/PDMS and PDMS/glass channels sufficiently reproducible and stable for chemical analysis (76).

One-dimensional (1D) SDS capillary gel electrophoresis (CGE) has also been performed in a microchannel (77) as well as 2D gel electrophoresis. The first dimension in 2D gel electrophoresis is IEF and the second dimension is SDS gel electrophoresis (78). Finally, PDMS channels can also be used to separate DNA. Since DNA fragments exhibit similar charge/mass ratios despite differences in size, they separate poorly in an open channel. Doyle and co-workers (79) demonstrated the use of a stationary phase consisting of a self-assembled magnetic matrix for separating DNA in a PDMS channel. The device effectively separated large DNA fragments (10–50 kbp).

Sorting of Cells. The two most common methods for sorting and enriching cell populations are the fluorescence activated cell sorter and magnetic filtration. Both methods can be miniaturized to microfluidic formats.

Flow cytometry is a technique used for counting, examining, and sorting of suspended particles in a stream of fluid. By detecting light scattering at different angles and wavelengths for fluorescently labeled cells, flow cytometers can yield measurements of cell size and shape, DNA content, cell surface markers, cell cycle distribution, and viability. In conventional flow cytometry, a sheath fluid flow surrounding the cells allows the cells to move into a single file format so that the cells can be examined one at a time. The same sheath flow concept can be realized in microfluidics via laminar flow by using a buffer that flows from side channels into the cell-transporting channel (Fig. 6). This flow-pinching method enhances the detection of single particles without clogging of the channel, a potential complication in an alternative method of focusing by narrowing the channel itself. Integrating the output of microfabricated flow cytometers directly with microfluidic polymerase chain reaction (PCR) chips, DNA sequencing chips, and systems for analyzing single protein molecules may facilitate quick, direct, and automated analysis of the contents of a cell (81). Disadvantages of microfabricated cell sorters compared to conventional FACS (fluorescence activated cell sorter) include the low throughput of sorting and a low recovery of viable cells.

An alternative technique to flow cytometry is magnetic cell sorting. Target cells are labeled with antibody-coated superparamagnetic beads (50 nm to $3\,\mu$m), and the mixture is passed through a separation column. Typically, the separation column contains ferromagnetic collection elements that act as field concentrators to retain the labeled cells on the column. The column is washed, the magnetic field is removed, and the retained cells are eluted. In a miniaturized
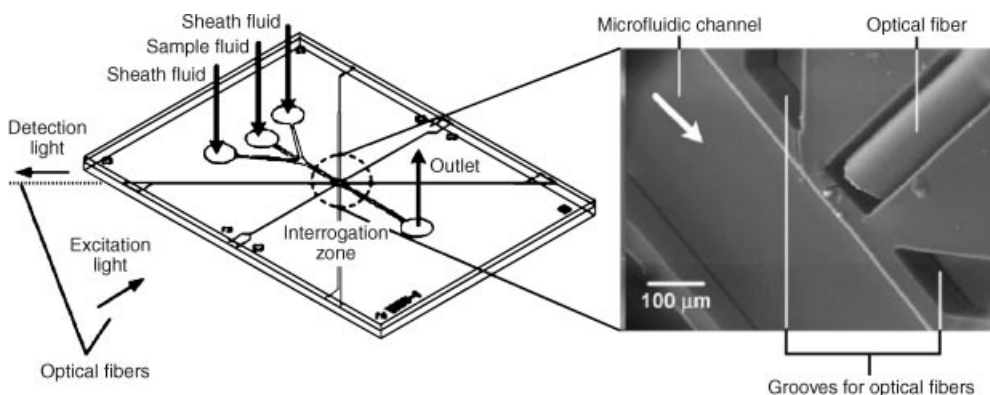
Fig. 6. Schematic diagram and micrograph of a microfabricated PDMS flow cytometer with embedded optical-fiber waveguides. Optical fibers are inserted close to a microfluidic channel through microfabricated grooves. Using lasers and photodetectors, samples flowing in the observation zone are excited and detected at multiple angles, permitting multicolor sample detection. [Reprinted with permission from Elsevier (80).]

format of magnetic cell sorting, a permanent magnet can be placed next to the microchannel to generate a magnetic field and induce separation. One approach featured a magnetic filtration system with 15-μm diameter nickel posts that act as magnetic field concentrators in the presence of an external magnetic field to separate 4.5-μm beads (82). The device efficiently separated 95% of the paramagnetic beads from diamagnetic beads. The system has thus far not been used to separate and sort magnetically tagged cells.

In a third technique, DEP (dielectrophoresis)-based cell separation methods are now widely in use. It uses electric fields to manipulate DNA, viruses, proteins, and cells. In DEP, nonuniform alternating current (ac) electric fields impart a polarization and lateral motion on uncharged particles. For multiple cell types, it is possible to identify specific frequencies that strongly attract one specific kind of cell, while imparting a smaller attractive DEP force (or even negative DEP forces) to other cell types (83,84). In one example, DEP has been demonstrated in a microfluidic device as an effective method for discriminating between infected and uninfected blood cells at concentrations of <1 infected cell per 100 normal cells (85).

Cell Patterning. Cell patterning is an important technique for cell-based biosensors, tissue engineering, and fundamental studies of cell biology. Photolithography on hard materials, such has borosilicate wafers, has been widely used (86–88). Cell-adhesion proteins, such as polylysine, fibronectin, and collagen, are applied on photoresist patterns and lifted off by sonication in acetone. The material is then incubated with growth medium, and the desired cell pattern can be obtained. This technique has disadvantages for biological applications since many chemicals used in this method are toxic to cells. Also, biological solutions are banned from the cleanroom because certain ions and molecules harm the conductivity of a semiconductor circuit (89).

Soft lithography with PDMS has been used to overcome these problems. The PDMS is biocompatible, optically transparent, permeable to gases,
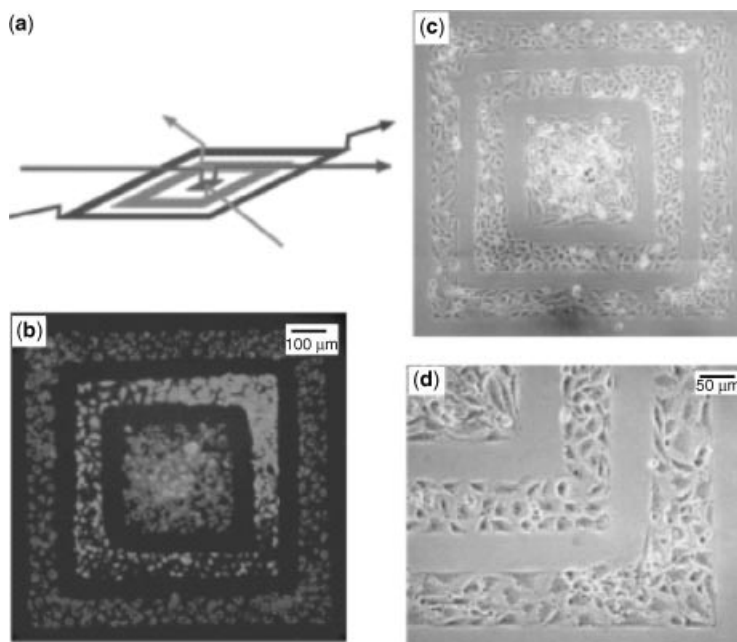
Fig. 7. Patterning of cells using microfluidics. Part (**a**) shows a schematic representation of a 3D PDMS stamp. Fluorescence (**b**) and phase-contrast (**c** and **d**) pictures of two cell types deposited on a tissue culture dish using the concentric square pattern in part (**a**). [Adapted with permission from The National Academy of Sciences (90).]

elastomeric, and durable. These features make it a suitable platform for miniaturized biological studies. By sealing PDMS microchannels on substrates, eg, glass, one can deliver materials for cell adhesion or cell suspension to desired areas. Using microfluidics, the size and shape of a cell-adhesive region can be manipulated on the surface of a cell-culture substrate (Fig. 7). In one study, researchers demonstrated the use of laminar flow of liquids to selectively pattern cell culture substrates with different proteins, pattern cells adjacent to each other, deliver chemicals to adhered cells, and perform enzymatic reactions over selected cells or over a portion of a cell (91).

In another approach, Langer and co-workers patterned arrays of nonbiofouling substances within microfluidic channels (78). The patterned arrays were used to fabricate arrays of proteins and of mammalian cells. The cells remained viable for 24 h, could perform intracellular reactions, and could be potentially lysed for analysis. Although there are other methods to pattern cells in 2D (eg, microstamping using PDMS molds), microfluidics makes it possible for researchers to engineer simple patterns with multiple-cell types (92).

3.4. Lab on a Chip.   A typical LOC device consists of a piece of palm-sized glass or plastic microfluidic chip with an external instrument for fluid processes and signal detection. It can perform integrated chemical and biomedical processes on a single chip, as in micro total analysis system (µTAS) that perform chemical analysis (Fig. 8). Compared to their traditional counterparts, such miniaturized devices need very small amounts of biological samples, can reduce
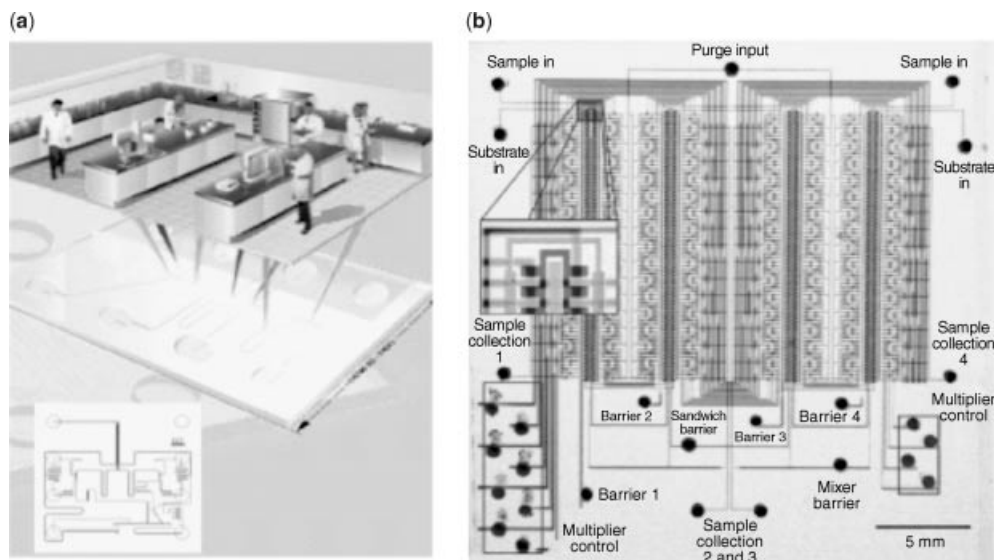
Fig. 8. Large-scale integration of microfluidics and LOC devices. (**a**) With a LOC, researchers can perform integrated chemical and biomedical processes with high quality and reproducibility on a single chip (93). (**b**) Optical micrograph of a microfluidic comparator chip. Different food dyes are loaded into various inputs to visualize the channels logic. [Reprinted with permission from AAAS (94).]

operation and analysis time by deploying parallel processes, and also increase integration and portability. Therefore, the use of microfluidic chips can significantly reduce the cost of chemical and biological reagents. Applications include environmental monitoring, point-of-care diagnostics, and drug screening processes.

Since devices used in real practice require multiple discrete experimental steps (eg, sample pretreatment, separation, enzymatic reactions, filtration, and detection), researchers are attempting to make LOC technologies modular such that they can be easily integrated onto a single LOC device. Quake and co-workers demonstrated stepwise synthesis of an [^{18}F]fluoride-radiolabeled molecular imaging probe ([^{18}F]FDG), in an integrated microfluidic device. Five sequential processes—[^{18}F]fluoride concentration, water evaporation, radiofluorination, solvent exchange, and hydrolytic deprotection—were carried out sequentially and automated by a computer programmed (LabVIEW) interface to operate the device (95). In a recent development, microfluidic components and microelectronic integrated circuits were combined as miniaturized easy-to-use LOCs (96). Use of integrated circuits (IC) provides flexibility for the end user who can perform different bioassays on the same chip by plugging in the required IC modules. The increasing complexity of applications has led microfluidic LOCs to become more modular both in terms of combining multiple steps in the same chip, and integrating chips with existing laboratory instrumentation and equipment.

Recent advances in LOC technologies have enhanced the feasibility of autonomous chemical and biochemical analyzers. Mathies has developed a device that uses microfabricated pumps and sippers to obtain environ mental samples (eg, an aqueous extract of solids) via a cryobot. This group is developing devices that will analyze a large variety of bioorganic molecules; this capability may allow devices to detect bioorganic molecules in extraterrestrial bodies, such as asteroids, Mars, and Europa, a moon of the planet Jupiter (97).

Valves. A key enabling technology in developing sophisticated LOC devices is the fabrication of valves. A valve is typically a membrane that can be finely controlled and that is used to stop, start, or regulate the flow of liquid through a microchannel. Although silicon- and glass-based materials are widely adopted in electronic and mechanical devices, their intrinsic stiffness poses a difficulty for making devices with moving parts for applications in biology and chemistry that require fluidic control.

Multilayer soft lithography is an excellent alternative for microfabrication of valves, and was first realized by Quake's group for this purpose (98,99). This technique uses a cross-channel architecture made of PDMS to fabricate a pneumatically actuated valve. In this design, pressure is applied to the upper channel to deflect a thin PDMS membrane downward; this deflection closes the lower, rounded channel and stops fluid flow (98). In another study, an elastomeric switch in a PDMS system featuring two crossing channels, each in a different layer, was demonstrated (100). Application of an external pressure above and below the crossing of the channel decreases the aspect ratio at the crossing, such that the fluid turns into the other channel due to lower fluidic resistance, instead of flowing straight through the crossing. In addition, pneumatically actuated PDMS valves can also be combined with glass microfluidic channels (101). Advantages of pneumatically actuated valves include ease of fabrication (by multistep lithography), rapid response time, avoidance of air bubbles, and compatibility with a large number of fluids. With these techniques, an integrated high density microfluidic chip with thousands of micromechanical valves and hundreds of individually addressable chambers can be built (94). These fluidic devices are analogous to electronic integrated circuits, in that a combinatorial array of binary valve patterns functions as a fluidic multiplexer. For example, these integrated microfluidic networks can be constructed to resemble a random-access memory (RAM) (95).

There are also other approaches for constructing valves (36,102–104). Torque-actuated valves consist of small machine screws ($\sim$500-µm diameter) rooted in a layer of polyurethane and placed over PDMS microfluidic channels. Valves featuring piezoelectric actuation make use of the electrically induced mechanical deformation of a piezoelectric material. Electrochemical valves operate on the principle that the application of a potential to an electrolytic solution forces a phase-change reaction to deflect membranes. Hydrogels can act as valves since they undergo abrupt volume changes in response to the stimuli without external power source, although they are difficult to integrate with microfluidics at the microscale. Beebe and co-workers reported an approach by combining lithography, photopolymerization and microfluidics to form valves inside microchannels (105). The hydrogel valves showed a good response time ($<$10 s), and are capable of autonomous control of local flow.

4. Industrial Impact

Due to the clear potential of using microfluidics for real-world applications and devices, commercialization of microfluidic technology began soon after the initial research developments at universities (106). In 1995, Ramsey founded the first (and currently the biggest) company in microfluidics, Caliper Life Sciences. Together with Agilent, Caliper developed one of the first commercial LOC systems. Currently, the company focuses on electrophoretic separation of proteins, nucleic acids, and other molecules on glass chips, and offers a drug screening system using high throughput kinase assays. Fluidigm is another important company in microfluidics. The company uses the PDMS valves developed by Quake to build integrated fluidic chips. Its first product was launched in 2003 for parallel testing of protein crystallization conditions. For microfluidic systems geared toward use in the research market, an attractive feature for end users is potentially increased analytical performance with very low consumption of precious reagents.

Other companies in the microfluidics field are focusing on building devices for use outside of the research laboratory. Cepheid has developed a microfluidic system that performs real-time PCR in order to detect DNA in anthrax spores (reportedly with a limit of detection of 30 spores). Other companies are focusing on developing microfluidic systems for the analysis of nucleic acids; examples include MicroFluidic Systems (which has developed a product that lyses cells to release their DNA content) and Handylab (which is developing a low cost microfluidic PCR system). For microfluidic systems to be used widely (eg, for consumer use), the cost of both the instrument and the chip will have to be decreased substantially without sacrificing simplicity of use. One current effort to this end is a collaboration between Yager's group and Micronics (which develops laminate microfluidic chips in Mylar), with the support of the Gates Foundation, to develop a low cost microfluidic system for diagnostic use in developing countries. Another effort toward the goal of low cost, POC microfluidic systems is being spearheaded by Claros Diagnostics.

5. Future Directions

Microfluidics provides researchers with a powerful platform for exploring and exploiting scientific phenomena in a precise and controlled manner. It reduces the time and cost of common assays, and enables the study of biological samples in detail. Great progress has been made in microfluidic technology over the last decade in academic and commercial laboratories, and the benefits of miniaturization are being realized across a number of scientific fields. Several key challenges must be met, however, in order to build a functional LOC. These challenges include the following: (*1*) building a seamless world-to-chip interface; (*2*) developing methods for pretreating "real-world" samples (from the laboratory, body or field), for handling fluids on-chip, and for minimizing clogging of microchannels due to small particles of dust or sample precipitation; (*3*) integrating multiple microfluidic components and assays (each with different requirements for buffer and running conditions); (*4*) reducing the cost in the liquid handling instrument,

detector, and microfluidic chip. While liquid economy has been the leading advantage for microfluidics, this characteristic also brings some drawbacks: it requires a sensitive method of detection (which imposes a significant limitation for dilute samples) and has a very limited capacity for preparative work. Nonetheless, potential applications are many, giving rise to miniaturized bioanalytical instruments, medical diagnostic devices, and high throughput methods for drug screening, protein crystallization, gene-expression profiling, proteomics, and combinatorial assays.

BIBLIOGRAPHY

1. A. Manz, J. Miyahara, J. Miura, Y. Watanabe, H. Miyagi, and K. Sato, *Sensors Actuators B* **1**, 249 (1990).
2. A. Manz, N. Graber, and H. M. Widmer, *Science* **1**, 244 (1990).
3. D. J. Harrison, K. Fluri, K. Seiler, Z. Fan, C. S. Effenhauser, and A. Manz, *Science* 895 (1993).
4. S. C. Terry, J. H. Jerman, and J. B. Angell, *IEEE Trans. Elect. Devices* **ED-26**, 1880 (1979).
5. A. Manz and J. C. T. Eijkel, *Pure Appl. Chem.* **73**, 1555 (2001).
6. F. M. White, *McGraw-Hill Science/Engineering/Math*, New York, 2005.
7. R. B. Bird, W. E. Stewart, and E. N. Lightfoot, *Trans. Phenom.*, John Wiley & Sons, Inc., New York, 2001.
8. A. Hatch, A. E. Kamholz, K. R. Hawkins, M. S. Munson, E. A. Schilling, B. H. Weigl, and P. Yager, *Nat. Biotechnol.* **19**, 461 (2001).
9. B. H. Weigl and P. Yager, *Science* **283**, 346 (1999).
10. R. Ferrigno, A. D. Stroock, T. D. Clark, M. Mayer, and G. M. Whitesides, *J. Am. Chem. Soc.* **124**, 12930 (2002).
11. P. J. Kenis, R. F. Ismagilov, and G. M. Whitesides, *Science* **285**, 83 (1999).
12. P. J. Kenis, R. F. Ismagilov, S. Takayama, G. M. Whitesides, S. Li, and H. S. White, *Acc. Chem. Res.* **33**, 841 (2000).
13. S. Takayama, E. Ostuni, P. LeDuc, K. Naruse, D. E. Ingber, and G. M. Whitesides, *Nature* (*London*) **411**, 1016 (2001).
14. H. C. Berg, *Random Walks in Biology*, Princeton University Press, Princeton, N.J., 1993.
15. N. A. Mortensen, F. Okkels, and H. Bruus, *Phys. Rev. E Stat. Nonlin. Soft Matter. Phys.* **71**, 057301 (2005).
16. F. M. White, *Viscous Fluid Flow*, McGraw-Hill, Boston, 1991.
17. G. T. A. Kovacs, *Micromachined Transducers Sourcebook*, McGraw-Hill, Inc., New York, 1998.
18. J. Lee, H. Moon, J. Fowler, C. J. Kim, and T. Schoellhammer, *IEEE Workshop MEMS* 499 (2001).
19. W. Satoh, H. Hosono, and H. Suzuki, *Anal. Chem.* **77**, 6857 (2005).
20. M. Pollack, R. Fair, and A. Shenderov, *Appl. Phys. Lett.* (2000).
21. S. Ghosal, *Annu. Rev. Fluid Mech.* **38**, 309 (2006).
22. E. Delamarche, A. Bernard, H. Schmid, B. Michel, and H. Biebuyck, *Science* **276**, 779 (1997).
23. D. C. Duffy, H. L. Gillis, J. Lin, N. F. S., Jr., and G. J. Kellogg, *Anal. Chem.* **71**, 4669 (1999).
24. B. S. Gallardo and co-workers, *Science* **283**, 57 (1999).
25. D. E. Kataoka and S. M. Troian, *Nature* (*London*) **402**, 794 (1999).

26. D. Juncker and co-workers, *Anal. Chem.* **74**, 6139 (2002).

27. H. A. Stone, A. D. Stroock, and A. Ajdari, *Annu. Rev. Fluid Mech.* 381 (2004).

28. M. Gad-el-Hak, *The MEMS Handbook*, CRC Press, Boca Raton, Flor., 2002.

29. U. Wallrabe, P. Ruther, T. Schaller, and W. K. Schomburg, *Int. J. Artif. Organs* **21**, 137 (1998).

30. C. H. Lin, G. B. Lee, Y. H. Lin, and G. L. Chang, *J. Micromech. Microeng.* **11**, 726 (2001).

31. M. J. Duffy, O. J. A. Schueller, and G. M. Whitesides, *Anal. Chem.* **70**, 4974 (1998).

32. J. C. McDonald and co-workers, *Electrophoresis* **21**, 27 (2000).

33. I. G. Jessamine, M. K. Ng, A. D. Stroock, and G. M. Whitesides, *Electrophoresis* **23**, 3461 (2002).

34. V. Linder, H. Wu, X. Jiang, and G. M. Whitesides, *Anal. Chem.* **75**, 2522 (2003).

35. N. Lee and G. M. Whitesides, *Anal. Chem.* **75**, 6544 (2004).

36. D. B. Weibel, M. Kruithof, S. Potenta, S. K. Sia, A. Lee, and G. M. Whitesides, *Anal. Chem.* **77**, 4726 (2005).

37. C. A. Davidson and C. R. Lowe, *J. Mol. Recognit.* **17**, 180 (2004).

38. D. Belder and M. Ludwig, *Electrophoresis* **24**, 3595 (2003).

39. A. V. Lemoff and A. P. Lee, *Sensors Actuators B* **63**, 178 (2000).

40. L. H. Lu, K. S. Ryu, and C. Liu, *J. Microelectromech. Syst.* **11**, 462 (2002).

41. A. D. Stroock, S. K. W. Dertinger, A. Adjari, I. Mezic, H. A. Stone, and G. M. Whitesides, *Science* **295**, 647 (2002).

42. A. Groisman and V. Steinberg, *Nature* (*London*) **410**, 905 (2001).

43. P. Garstecki, M. A. Fischbach, S. K. Sia, and G. M. Whitesides, *Lab Chip* **6**, 207 (2006).

44. J.-W. Choi and C. H. Ahn, *Solid-State Sensor Actuator Workshop* 52 (2000).

45. M. H. Oddy, J. G. Santiago, and J. C. Mikkelsen, *Anal. Chem.* **73**, 5822 (2001).

46. T. Squires and S. Quake, *Rev. Mod. Phys.* **77**, 977 (2005).

47. D. R. Link and co-workers, *Angew. Chem. Int. Ed. Engl.* **45**, 2556 (2006).

48. H. Song, J. D. Tice, and R. F. Ismagilov, *Angew. Chem. Int. Ed. Engl.* **42**, 768 (2003).

49. A. D. Stroock and co-workers, *Phys. Rev. Lett.* **84**, 3314 (2000).

50. H. Song and R. F. Ismagilov, *J. Am. Chem. Soc.* **125**, 14613 (2003).

51. H. Mao, T. Yang, and P. S. Cremer, *J. Am. Chem. Soc.* **124**, 4432 (2002).

52. H. Mao, M. A. Holden, M. You, and P. S. Cremer, *Anal. Chem.* **74**, 5071 (2002).

53. A. Bernard, B. Michel, and E. Delamarche, *Anal. Chem.* **73**, 8 (2001).

54. S. K. Sia, V. Linder, B. A. Parviz, A. Siegel, and G. M. Whitesides, *Angew. Chem. Int. Ed. Engl.* **43**, 498 (2004).

55. V. Linder, S. K. Sia, and G. M. Whitesides, *Anal. Chem.* **77**, 64 (2005).

56. L. Ceriotti and co-workers, *Electrophoresis* **23**, 3615 (2002).

57. A. Ramseier, F. von Heeren, and W. Thormann, *Electrophoresis* **19**, 2967 (1998).

58. B. Zhang, F. Foret, and B. L. Karger, *Anal. Chem.* **72**, 1015 (2000).

59. C. S. Effenhauser, A. Manz, and H. M. Widmer, *Anal. Chem.* **67**, 2284 (1995).

60. Y. Liu, R. S. Foote, S. C. Jacobson, R. S. Ramsey, and J. M. Ramsey, *Anal. Chem.* **72**, 4608 (2000).

61. Y. Shi and co-workers, *Anal. Chem.* **71**, 5354 (1999).

62. N. A. Lacher, N. F. de Rooij, E. Verpoorte, and S. M. Lunte, *J. Chromatogr. A* **1004**, 225 (2003).

63. D. S. Reichmuth, T. J. Shepodd, and B. J. Kirby, *Anal. Chem.* **76**, 5063 (2004).

64. C. M. Harris, *Anal. Chem.* **75**, 64A (2003).

65. M. Vazquez and co-workers, *J. Chromatogr. B Anal. Technol. Biomed. Life Sci.* **779**, 163 (2002).

66. O. Mueller, K. Hahnenberger, M. Dittmann, H. Yee, R. Dubrow, R. Nagle, and D. Ilsley, *Electrophoresis* **21**, 128 (2000).

67. J. C. Eijkel, A. van den Berg, and A. Manz, *Electrophoresis* **25**, 243 (2004).
68. D. J. Harrison, A. Manz, Z. Fan, H. Ludi, and H. M. Widmer, *Anal. Chem.* **64**, 1926 (1992).
69. A. Manz and co-workers, *J. Chromatogr.* **593**, 253 (1992).
70. C. X. Zhang and A. Manz, *Anal. Chem.* **75**, 5759 (2003).
71. J. D. Ramsey, S. C. Jacobson, C. T. Culbertson, and J. M. Ramsey, *Anal. Chem.* **75**, 3758 (2003).
72. A. E. Herr, J. I. Molho, K. A. Drouvalakis, J. C. Mikkelsen, P. J. Utz, J. G. Santiago, and T. W. Kenny, *Anal. Chem.* **75**, 1180 (2003).
73. B. G. Effenhauser, A. Paulus, and M. Ehrat, *Anal. Chem.* **69**, 3451 (1997).
74. G. Ocvirk, M. Munroe, T. Tang, R. Oleschuk, K. Westra, and D. J. Harrison, *Electrophoresis* **21**, 107 (2000).
75. X. Ren, M. Bachman, C. Sims, G. P. Li, and N. Allbritton, *J. Chromatogr. B Biomed. Sci. Appl.* **762**, 117 (2001).
76. A. M. Spehar and co-workers, *Electrophoresis* **24**, 3674 (2003).
77. S. Yao, D. S. Anex, W. B. Caldwell, D. W. Arnold, K. B. Smith, and P. G. Schultz, *Proc. Natl. Acad. Sci. U. S. A.* **96**, 5372 (1999).
78. A. Khademhosseini, K. Y. Suh, S. Jon, G. Eng, J. Yeh, G. J. Chen, and R. Langer, *Anal. Chem.* **76**, 3675 (2004).
79. P. S. Doyle, J. Bibette, A. Bancaud, and J. L. Viovy, *Science* **295**, 2237 (2002).
80. Y. Tung, M. Zhang, C. Lin, K. Kurabayashi, and S. Skerlos, *Sensors Actuators B* **98**, 356 (2004).
81. D. R. Meldrum and M. R. Holl, *Science* **297**, 1197 (2002).
82. T. Deng, M. Prentiss, and G. M. Whitesides, *Appl. Phys. Lett.* **80**, 461 (2002).
83. L. M. Broche, F. H. Labeed, and M. P. Hughes, *Phys. Med. Biol.* **50**, 2267 (2005).
84. J. Voldman, *Annu. Rev. Biomed. Eng.* (2006).
85. P. Gascoyne, C. Mahidol, M. Ruchirawat, J. Satayavivad, P. Watcharasit, and F. F. Becker, *Lab Chip* **2**, 70 (2002).
86. D. Kleinfeld, K. H. Kahler, and P. E. Hockberger, *J. Neurosci.* **8**, 4098 (1988).
87. S. N. Bhatia, M. L. Yarmush, and M. Toner, *J. Biomed. Mater. Res.* **34**, 189 (1997).
88. K. E. Healy, C. H. Thomas, A. Rezania, J. E. Kim, P. J. McKeown, B. Lom, and P. E. Hockberger, *Biomaterials* **17**, 195 (1996).
89. T. H. Park and M. L. Shuler, *Biotechnol. Prog.* **19**, 243 (2003).
90. D. T. Chiu and co-workers, *Proc. Natl. Acad. Sci. U. S. A.* **97**, 2408 (2000).
91. S. Takayama and co-workers, *Proc. Natl. Acad. Sci. U. S. A.* **96**, 5545 (1999).
92. A. Khademhosseini, R. Langer, J. Borenstein, and J. P. Vacanti, *Proc. Natl. Acad. Sci. U. S. A.* **103**, 2480 (2006).
93. SATS-Symposium-Ryan, Una (2004, May 7). Australian Academy of Science. Available at http://www.science.org.au/sats2004/ryan.htm.
94. T. Thorsen, S. J. Maerkl, and S. R. Quake, *Science* **298**, 580 (2002).
95. C. C. Lee and co-workers, *Science 310*, 1793 (2005).
96. H. Lee, Y. Liu, E. Alsberg, D. E. Ingber, R. M. Westervelt, and D. Ham, *IEEE Int. Solid State Circuits* (2005).
97. A. M. Skelley and co-workers, *Proc. Natl. Acad. Sci. U. S. A.* **102**, 1041 (2005).
98. M. A. Unger, H.-P. Chou, T. Thorsen, A. Scherer, and S. R. Quake, *Science* **288**, 113 (2000).
99. S. R. Quake and A. Scherer, *Science* **290**, 1536 (2000).
100. R. F. Ismagilov and co-workers, *Anal. Chem.* **73**, 4682 (2001).
101. W. H. Grover, A. M. Skelley, C. N. Liu, E. T. Lagally, and R. A. Mathies, *Sensors Actuators B* **89**, 315 (2003).

102. R. Duggirala and A. Lal. 2003. Presented at the Digest of Technical publications, The 12th International Conference on Solid State Sensors, Actuators and + Micro-systems, Transducers'03, Boston.
103. P. Griss, H. Andersson, and G. Stemme, *Lab Chip* **2**, 117 (2002).
104. S. Z. Hua, F. Sachs, D. X. Yang, and H. D. Chopra, *Anal. Chem.* **74**, 6392 (2002).
105. D. J. Beebe, J. S. Moore, J. M. Bauer, Q. Yu, R. H. Liu, C. Devadoss, and B. H. Jo, *Nature* (*London*) **404**, 588 (2000).
106. M. M. Stephan, *The Scientist* **19**, 43 (2005).

JERRY LII
WERN-JIR HSU
STEPHANIE P. LEE
SAMUEL K. SIA
Columbia University